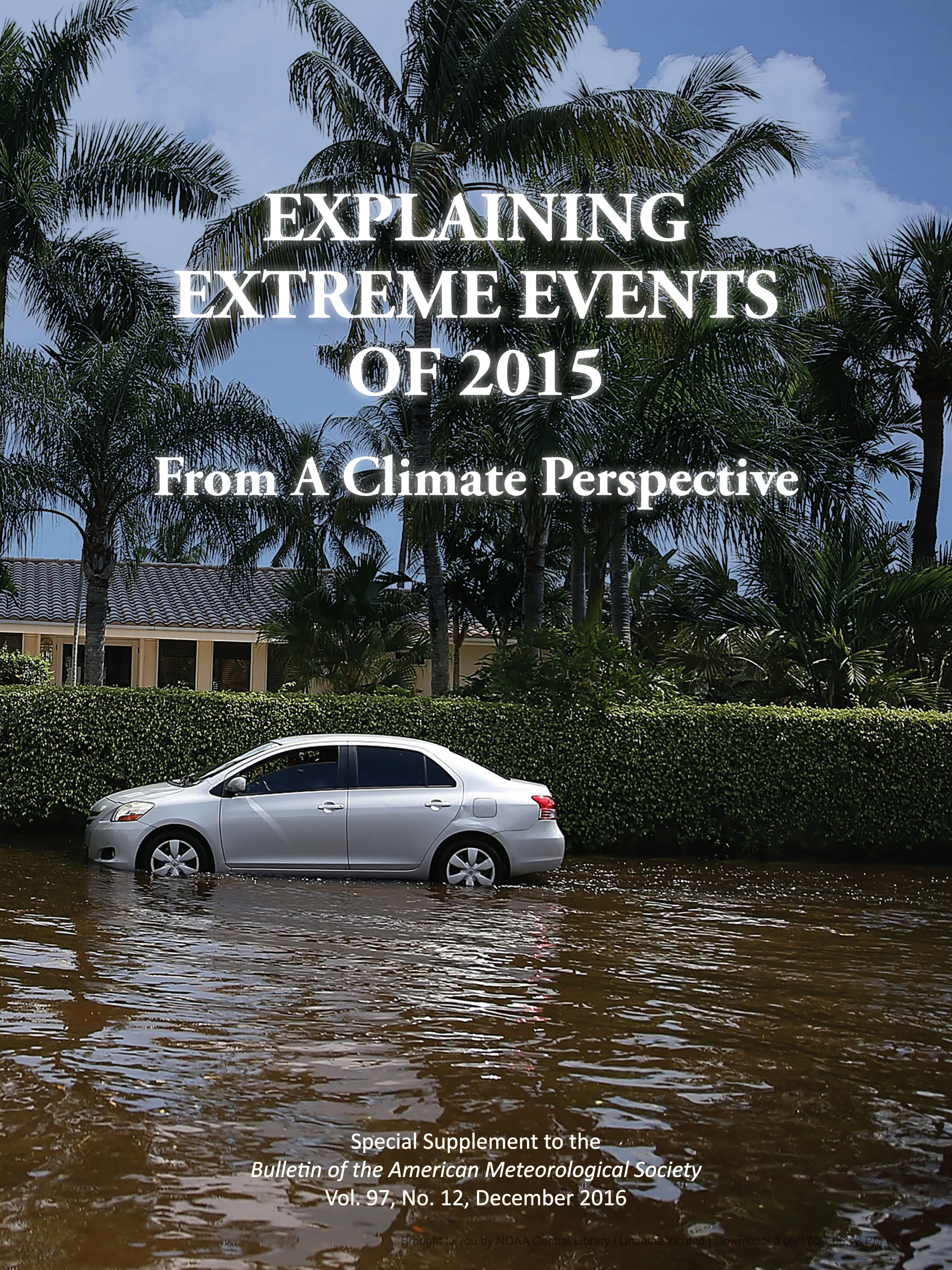

EXPLAINING EXTREME EVENTS OF 2015

From A Climate Perspective

Special Supplement to the
Bulletin of the American Meteorological Society
Vol. 97, No. 12, December 2016

EXPLAINING EXTREME EVENTS OF 2015 FROM A CLIMATE PERSPECTIVE

Editors

Stephanie C. Herring, Andrew Hoell, Martin P. Hoerling, James P. Kossin, Carl J. Schreck III, and Peter A. Stott

Special Supplement to the

Bulletin of the American Meteorological Society

Vol. 97, No. 12, December 2016

American Meteorological Society

Corresponding Editor:

Stephanie C. Herring, PhD
NOAA National Centers for Environmental Information
325 Broadway, E/CC23, Rm 1B-131
Boulder, CO, 80305-3328
E-mail: stephanie.herring@noaa.gov

Cover Credit:

HOW TO CITE THIS DOCUMENT

Citing the complete report:

Herring, S. C., A. Hoell, M. P. Hoerling, J. P. Kossin, C. J. Schreck III, and P. A. Stott, Eds., 2016: Explaining Extreme Events of 2015 from a Climate Perspective. *Bull. Amer. Meteor. Soc.*, **97 (12)**, S1–S145.

Citing a section (example):

Partain, J. L., and Coauthors, 2016: An assessment of the role of anthropogenic climate change in the Alaska fire season of 2015 [in "Explaining Extremes of 2015 from a Climate Perspective"]. *Bull. Amer. Meteor. Soc.*, **97 (12)**, S14–S18, doi:10.1175/BAMS-D-16-0149.

EDITORIAL AND PRODUCTION TEAM

Riddle, Deborah B., Lead Graphics Production, NOAA/NESDIS National Centers for Environmental Information, Asheville, NC

Veasey, Sara W., Visual Communications Team Lead, NOAA/NESDIS National Centers for Environmental Information, Asheville, NC

Love-Brotak, S. Elizabeth, Graphics Support, NOAA/NESDIS National Centers for Environmental Information, Asheville, NC

Fulford, Jennifer, Editorial Support, Telesolv Consulting LLC, NOAA/NESDIS National Centers for Environmental Information, Asheville, NC

Griffin, Jessicca, Graphics Support, Cooperative Institute for Climate and Satellites-NC, North Carolina State University, Asheville, NC

Maycock, Tom, Editorial Support, Cooperative Institute for Climate and Satellites-NC, North Carolina State University, Asheville, NC

Misch, Deborah J., Graphics Support, Telesolv Consulting LLC, NOAA/NESDIS National Centers for Environmental Information, Asheville, NC

Osborne, Susan, Editorial Support, Telesolv Consulting LLC, NOAA/NESDIS National Centers for Environmental Information, Asheville, NC

Sprain, Mara, Editorial Support, LAC Group, NOAA/NESDIS National Centers for Environmental Information, Asheville, NC

Young, Teresa, Graphics Support, STG, Inc., NOAA/NESDIS National Centers for Environmental Information, Asheville, NC

TABLE OF CONTENTS

ABSTRACT—

Stephanie C. Herring, Andrew Hoell, Martin P. Hoerling, James P. Kossin, Carl J. Schreck III, and Peter A. Stott

This fifth edition of explaining extreme events of the previous year (2015) from a climate perspective continues to provide evidence that climate change is altering some extreme event risk. Without exception, all the heat-related events studied in this year's report were found to have been made more intense or likely due to human-induced climate change, and this was discernible even for those events strongly influenced by the 2015 El Niño. Furthermore, many papers in this year's report demonstrate that attribution science is capable of separating the effects of natural drivers including the strong 2015 El Niño from the influences of long-term human-induced climate change.

Other event types investigated include cold winters, tropical cyclone activity, extreme sunshine in the United Kingdom, tidal flooding, precipitation, drought, reduced snowpack in the U.S. mountain west, arctic sea ice extent, and wildfires in Alaska. Two studies investigated extreme cold waves and monthly-mean cold conditions over eastern North America during 2015, and find these not to have been symptomatic of human-induced climate change. Instead, they find the cold conditions were caused primarily by internally generated natural variability. One of these studies shows winters are becoming warmer, less variable, with no increase in daily temperature extremes over the eastern United States. Tropical cyclone activity was extreme in 2015 in the western North Pacific (WNP) as measured by accumulated cyclone energy (ACE). In this report, a study finds that human-caused climate change largely increased the odds of this extreme cyclone activity season. The 2015 Alaska fire season burned the second largest number of acres since records began in 1940. Investigators find that human-induced climate change has increased the likelihood of a fire season of this severity.

Confidence in results and ability to quickly do an attribution analysis depend on the "three pillars" of event attribution: the quality of the observational record, the ability of models to simulate the event, and our understanding of the physical processes that drive the event and how they are being impacted by climate change. A result that does not find a role for climate change may be because one or more of these three elements is insufficient to draw a clear conclusion. As these pillars are strengthened for different event types, confidence in the presence and absence of a climate change influence will increase.

This year researchers also link how changes in extreme event risk impact human health and discomfort during heat waves, specifically by looking at the role of climate change on the wet bulb globe temperature during a deadly heat wave in Egypt. This report reflects a growing interest within the attribution community to connect attribution science to societal impacts to inform risk management through "impact attribution." Many will watch with great interest as this area of research evolves in the coming years.

26. INFLUENCES OF NATURAL VARIABILITY AND ANTHROPOGENIC FORCING ON THE EXTREME 2015 ACCUMULATED CYCLONE ENERGY IN THE WESTERN NORTH PACIFIC

Wei Zhang, Gabriel A. Vecchi, Hiroyuki Murakami, Gabriele Villarini, Thomas L. Delworth, Karen Paffendorf, Rich Gudgel, Liwei Jia, Fanrong Zeng, and Xiaosong Yang

The extreme value of the 2015 western North Pacific (WNP) accumulated cyclone energy (ACE) was mainly caused by the sea surface warming in the eastern and central Pacific, with the anthropogenic forcing largely increasing the odds of the occurrence of this event.

Introduction. The 2015 tropical cyclone (TC) activity measured by the ACE [computed as the sum of the square of the maximum surface wind speed (MSW) over the TC duration when MSW is greater than 34 knots; e.g., Bell et al. 2000] was extremely high in the western North Pacific Ocean (Figs. 26.1a,b and 26.2a). The 2015 WNP ACE is the second highest since 1970 (with the highest being 1997) based on the Joint Typhoon Warning Center best track data for 1970–2014 and Unisys data for 2015 (http://weather.unisys.com/hurricane/), the highest since 1977 based on the Japan Meteorological Agency (JMA), and the highest since 1970 based on Shanghai Typhoon Institute (STI) data. Higher (lower) WNP ACE is generally observed during El Niño (La Niña) years, because TCs are formed more southeastward (northwestward) and stay longer (shorter) over the warm ocean surface (e.g., Camargo and Sobel 2005; Chan 2007). This shift in genesis and difference in tracks leads to a higher occurrence of the most intense typhoons, which is the main cause of a high ACE during El Niño years. An extremely strong El Niño event developed in 2015. While there has been major progress in the understanding of the El Niño–Southern Oscillation (ENSO)–WNP ACE association, the modulation of WNP ACE by anthropogenic forcing is still a challenging scientific question (e.g., Emanuel 2013; Lin and Chan 2015). Using observations and a suite of climate model experiments, this study attempts to assess whether and to what extent internal climate modes (e.g., ENSO) and anthropogenic forcing contributed to the extreme 2015 WNP ACE event.

AFFILIATIONS: Zhang, Veechi, Murakami, Delworth, Paffendorf, Jia, and Yang—NOAA/Geophysical Fluid Dynamics Laboratory, Princeton, New Jersey; Zhang, Veechi, Murakami, Delworth, Paffendorf, Gudgel, Jia, and Zeng—Atmospheric and Oceanic Sciences Program, Princeton University, Princeton, New Jersey; Zhang and Villarini—IIHR–Hydroscience & Engineering, The University of Iowa, Iowa City, Iowa; Yang—University Corporation for Atmospheric Research, Boulder, Colorado

DOI:10.1175/BAMS-D-16-0146.1

A supplement to this article is available online (10.1175/BAMS-D-16-0146.2)

Methodology. We use two coupled general circulation models (CGCMs): the Geophysical Fluid Dynamics Laboratory (GFDL) forecast-oriented low ocean resolution model (FLOR; Vecchi et al. 2014) and high-resolution FLOR (HiFLOR; Murakami et al. 2015a; Zhang et al. 2016b). TCs are identified and tracked using a tracking algorithm based on various model variables (Zhang et al. 2016a,b; see online Supplemental Material). The climatological values of WNP ACE in the observations, FLOR, and HiFLOR are different partly because of different spatial resolutions and climate mean states; we therefore analyze the WNP ACE values in terms of exceedance probabilities (e.g., 0.95, 0.99) of all the sampled ACE values in observations and simulations. Following Murakami et al. (2015b) and Yang et al. (2015), we use a probabilistic approach to examine the probability of a WNP ACE event as:

$$P(x) = \frac{\text{Number of years with ACE} \geq x}{\text{Total number of years}} \quad (1)$$

where x is a selected WNP ACE value and $P(x)$ represents the probability with WNP ACE larger than or equal to x. We use the fraction of attributable risk (FAR; e.g., Allen 2003; Stott et al. 2004) to quantify the FAR to human influence or anthropogenic forcing. FAR is defined as FAR = 1 − (P_0/P_1), where P_0 (P_1) is the probability of exceeding the observed TC trend in the experiments without (with) anthropogenic forcing. We compute FAR using P_0 from a 1990 control experiment of FLOR and P_1 from a 2 × CO_2 experiment with the same model (van der Wiel et al. 2016). We also compute P_0 (P_1) from the two experiments of HiFLOR with radiative forcing representative of 1940 (2015; 1940 is also a strong El Niño year).

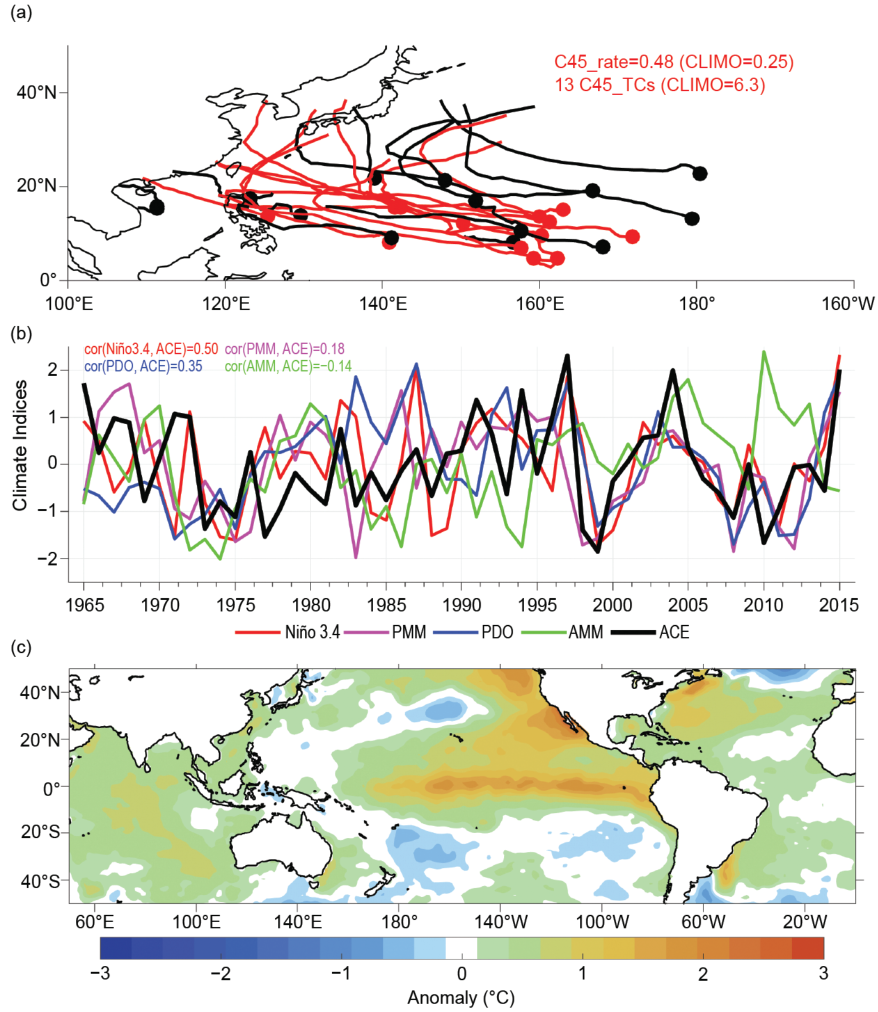

Fig. 26.1. (a) TC tracks in 2015 and C45 TCs (wind speed exceeding 58.1 m s⁻¹) are shown in red. The C45 proportion in 2015 is 0.48 while the climatology (1970–2015) is 0.26, with 13 (6.3) C45 TCs in 2015 (climatology; see Supplemental Material for data sources). (b) Time series of different annually averaged normalized climate indices (see legend) and ACE (black); Cor (Niño-3.4, ACE) denotes the correlation coefficient between Niño-3.4 index and WNP ACE for 1970–2015, while the others are defined likewise. (c) Sea surface temperature anomalies (°C) in 2015 computed with respect to the 1970–2000 base period.

Natural Variability. The extremely high 2015 WNP ACE is mostly due to a large number of category 4 and 5 (C45; wind speed exceeding 58.1 m s⁻¹) TCs (Fig. 26.1a). There were 13 C45 TCs in the WNP during 2015, more than twice the climatological value of 6.3. The 2015 C45 proportion, defined by the number of C45 TCs divided by the basin-total TCs, is 0.48 while the climatology (1970–2015) is 0.25. The 2015 basin-total TC frequency (27) is slightly higher than climatology (25). The ENSO–WNP ACE association is supported by the high Niño-3.4 index in 2015, similar to those in 1987 and 1997 (Figs. 26.1b,c). The SST warming in 2015 extends westward to 160°E, and this provides favorable conditions for TC intensification because WNP TC intensification is influenced both by TC genesis location and ocean temperature (Wada and Chan 2008; Mei et al. 2015; Zhang et al. 2015). Previous studies suggested that factors such as the Pacific meridional mode (PMM), the Pacific decadal oscillation (PDO), and the Atlantic meridional mode (AMM) (see Supplemental Material) may also modulate WNP ACE (e.g., Chan 2008; Zhang et al. 2016a,c). The correlations between WNP ACE and the Niño-3.4 (significant at 0.01 level), PMM (significant at 0.01 level), and PDO (not significant at the 0.01 level) indices are positive, while the correlation between WNP ACE and the AMM is negative but not statistically significant (Fig. 26.1b, see Supplemental Material for more details of the indices). The Niño-3.4 and PMM indices in 2015 are strongly positive, contributing to the extreme 2015 WNP ACE. Therefore, internal climate modes, especially the strong El Niño, may have substantially contributed to the extreme 2015 WNP ACE by leading to an extremely high frequency of C45 TCs (Camargo and Sobel 2005).

Effect of Anthropogenic Forcing. We analyze two sets of experiments (i.e., 1990 control and 2 × CO_2 experiments) with FLOR. The probability density functions

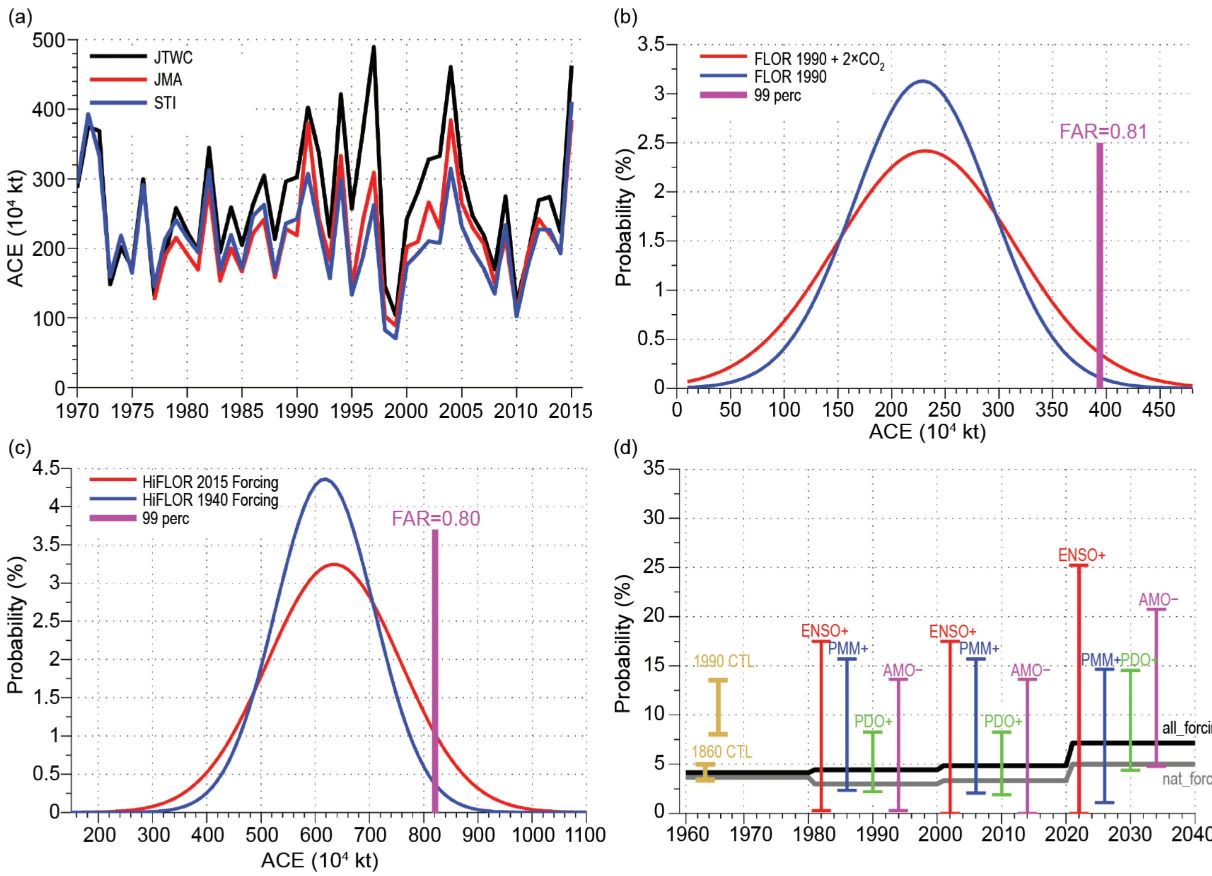

Fig. 26.2. (a) Annual WNP ACE based on observations. (b) PDFs of WNP ACE in 1990 (blue) and 2 × CO_2 (red) experiments with FLOR. (c) PDFs of WNP ACE in the experiments with radiative forcing representative of 1940 (blue) and 2015 (red) in HiFLOR. The magenta bars represent the 99th percentile of the ACE values (similar to observations) in FLOR/HiFLOR. (d) *P*(*x* = 95th percentile) in FLOR-FA all_forcing/nat_forcing multidecadal experiments with upper/lower limits of error bars represent ENSO+/− (red), PMM+/− (blue), PDO+/− (green), and AMO−/+ (magenta). The brown bars represent *P*(*x* = 95th percentile) in two control experiments with the widths representing the 0.95 confidence intervals. The black and gray curves represent *P*(*x* = 95th percentile) in samples of all_forcing and nat_forcing experiments, respectively.

(PDFs) of WNP ACE in FLOR 1990 control and 2 × CO_2 experiments have similar mean values while their variances are different, with a fatter tail in the 2 × CO_2 experiment (Fig. 26.2b). We select the ACE values in the 99th percentile of FLOR 1990 to calculate FAR, consistent with the percentile of the observed 2015 WNP ACE (Figs. 26.2a,b). The FAR in the 1990 control and 2 × CO_2 experiments of FLOR are 0.81, indicating that anthropogenic forcing can substantially increase the risk of having extreme WNP ACE events higher than or equal to the 2015 event. To further substantiate this finding, we also analyze P_0 and P_1 in the two experiments of HiFLOR with radiative forcing representative of 1940 and 2015. The PDFs of WNP ACE in HiFLOR also have a fatter tail in the experiment with radiative forcing representative of 2015 compared with that of 1940 (Fig. 26.2c). The FAR in HiFLOR is 0.80, close to 0.81 in the experiments with FLOR (Figs. 26.2b,c).

We ran 35-member simulations with all forcing (natural and anthropogenic under RCP 4.5 scenario) and 30-member multidecadal simulations with natural forcing from 1961 to 2040 (see Supplemental Material). For each 20-year period from 1961, 1300 (20 × 35 + 20 × 30) samples (years) were available to calculate $P(x)$. We define a simulated positive (or negative) phase of ENSO, PDO, PMM, and AMO as these indices exceeding (falling below) one (minus one) standard deviation and estimate the amplitude of $P(x)$ between the two phases. Figure 26.2d illustrates the results for $P(x = 95\text{th percentile})$. $P(x = 95\text{th}$ percentile$)$ in all_forcing experiments increases from 1960 to 2040, suggesting that the external forcing tends to increase the odds of occurrence of extreme

WNP ACE. There is a sharp increase in $P(x = 95\text{th percentile})$ during 2020–40 (Fig. 26.2d). In addition, the $P(x = 95\text{th percentile})$ in nat_forcing experiments also largely increases in 1960–2060, except for a slight decrease from 1960–80 to 1980–2000. The $P(x = 95\text{th percentile})$ in all_forcing experiments are higher than those in nat_forcing experiments, indicating that anthropogenic forcing increases the risk of having extreme WNP ACE events. The results based on FLOR-FA 1860 and 1990 control experiments are also shown in the left of Fig. 26.2d, providing additional support to these conclusions. For each 20-year subperiod in 1980–2040, ENSO produces the largest variability of WNP ACE (Fig. 26.2d). The variability associated with ENSO is larger than that associated with radiative forcing (Fig. 26.2d). Therefore, the extreme 2015 WNP ACE may be mainly modulated by natural climate modes, especially by the strong El Niño, with the anthropogenic forcing increasing the risk of 2015 having a season with an extremely high WNP ACE. This risk is predicted to continue to increase in the next few decades, increasing the probability of having seasons with a WNP ACE equal to or higher than 2015 in the future.

Discussions and Conclusions. We have observed an extremely active TC season in the WNP in 2015, with an extremely high ACE and frequency of C45 TCs. The 2015 season may be caused mainly by warm ocean surface temperatures in the tropical Pacific, characterized by a strong El Niño event, with other climate modes (e.g., PMM) potentially playing a role. We have found that anthropogenic forcing has substantially increased the risk of having WNP ACE higher than or equal to such an extreme event. Although the changes in WNP ACE under anthropogenic forcing are still unclear (e.g., Emanuel 2013; Lin and Chan 2015), both GFDL FLOR and HiFLOR do suggest that the annual WNP ACE tends to become more extreme because of anthropogenic forcing. The two models also suggest that the variability of WNP ACE attributable to climate modes will increase at a much higher rate than as a result of anthropogenic forcing. The frequency of strong El Niño events is projected to increase due to greenhouse warming (Cai et al. 2014), which in turn could potentially lead to a higher frequency of WNP seasons with high values of ACE.

ACKNOWLEDGEMENT. This material is based in part upon work supported by the National Science Foundation under Grants AGS-1262091 and AGS-1262099.

REFERENCES

Allen, M., 2003: Liability for climate change. *Nature*, **421**, 891–892.

Bell, G. D., and Coauthors, 2000: Climate assessment for 1999. *Bull. Amer. Meteor. Soc.*, **81 (6)**, S1–S50.

Cai, W., and Coauthors, 2014: Increasing frequency of extreme El Niño events due to greenhouse warming. *Nat. Climate Change*, **4**, 111–116, doi:10.1038/nclimate2100.

Camargo, S. J., and A. H. Sobel, 2005: Western North Pacific tropical cyclone intensity and ENSO. *J. Climate*, **18**, 2996–3006.

Chan, J. C. L., 2007: Interannual variations of intense typhoon activity. *Tellus*, **59A**, 455–460.

——, 2008: Decadal variations of intense typhoon occurrence in the western North Pacific. *Proc. Roy. Soc. London*, **464A**, 249–272.

Emanuel, K. A., 2013: Downscaling CMIP5 climate models shows increased tropical cyclone activity over the 21st century. *Proc. Natl. Acad. Sci. USA*, **110**, 12219–12224, doi:10.1073/pnas.1301293110.

Lin, I. I., and J. C. L. Chan, 2015: Recent decrease in typhoon destructive potential and global warming implications. *Nat. Commun.*, **6**, 7182, doi:10.1038/ncomms8182.

Mei, W., S.-P. Xie, F. Primeau, J. C. McWilliams, and C. Pasquero, 2015: Northwestern Pacific typhoon intensity controlled by changes in ocean temperatures. *Sci. Adv.*, **1**, e1500014, doi:10.1126/sciadv.1500014.

Murakami, H., and Coauthors, 2015a: Simulation and prediction of category 4 and 5 hurricanes in the high-resolution GFDL HiFLOR coupled climate model. *J. Climate*, **28**, 9058–9079. 10.1175/JCLI-D-15-0216.1.

——, G. A. Vecchi, T. L. Delworth, K. Paffendorf, L. Jia, R. Gudgel, and F. Zeng, 2015b: Investigating the influence of anthropogenic forcing and natural variability on the 2014 Hawaiian hurricane season [in "Explaining Extreme Events of 2014 from a Climate Perspective"]. *Bull. Amer. Meteor. Soc.*, **96 (12)**, S115–S119, doi:10.1175/BAMS-D-15-00119.1.

Stott, P. A., D. A. Stone, and M. R. Allen, 2004: Human contribution to the European heatwave of 2003. *Nature*, **432**, 610–614, doi:10.1038/nature03089.

Van der Wiel, K., and Coauthors, 2016: The resolution dependence of contiguous US precipitation extremes in response to CO_2 forcing. *J. Climate*, **29**, 7991–8012, doi:10.1175/JCLI-D-16-0307.1.

Vecchi, G. A., and Coauthors, 2014: On the seasonal forecasting of regional tropical cyclone activity. *J. Climate*, **27**, 7994–8016, doi:10.1175/JCLI-D-14-00158.1.
Wada, A., and J. C. L. Chan, 2008: Relationship between typhoon activity and upper ocean heat content. *Geophys. Res. Lett.*, **35**, L17603, doi:10.1029/2008GL035129.
Yang, X., G. A. Vecchi, T. L. Delworth, K. Paffendorf, R. Gudgel, L. Jia, S. D. Underwood, and F. Zeng, 2015: Extreme North America winter storm season of 2013/14: Roles of radiative forcing and the global warming hiatus [in "Explaining Extreme Events of 2014 from a Climate Perspective"]. *Bull. Amer. Meteor. Soc.*, **96 (12)**, S25–S28, doi:10.1175/BAMS-D-15-00133.1.
Zhang, W., Y. Leung, and K. Fraedrich, 2015: Different El Niño types and intense typhoons in the western North Pacific. *Climate Dyn.*, **44**, 2965–2977, doi:10.1007/s00382-014-2446-4.
——, and Coauthors, 2016a: The Pacific meridional mode and the occurrence of tropical cyclones in the western North Pacific. *J. Climate*, **29**, 381–398, doi:10.1175/JCLI-D-15-0282.1.
——, and Coauthors, 2016b: Improved simulation of tropical cyclone responses to ENSO in the western North Pacific in the high-resolution GFDL HiFLOR coupled climate model. *J. Climate*, **29**, 1391–1415, doi:10.1175/JCLI-D-15-0475.1.
——, G. A. Vecchi, G. Villarini, H. Murakami, A. Rosati, X. Yang, L. Jia, and F. Zengand, 2016c: Modulation of western North Pacific tropical cyclone activity by the Atlantic meridional mode. *Climate Dyn.*, in press, doi:10.1007/s00382-016-3099-2.

Table 28.1. Summary of Results

	ANTHROPOGENIC INFLUENCE ON EVENT		
	INCREASE	**DECREASE**	**NOT FOUND OR UNCERTAIN**
Heat	**Global Temperature** (Ch. 2) **South India & Sri Lanka** (Ch. 2) **Central Europe** (Ch. 11) **Europe** (Ch. 12) **Ethiopia and Southern Africa** (Ch. 15) **N.W. China** (Ch. 19) **W. China** (Ch. 20) **Japan** (Ch. 21) **Indonesia** (Ch. 22) **S. Australia** (Ch. 23) **Australia** (Ch. 24)		**Central Equitorial Pacific** (Ch. 2)
Cold		**Northeastern U.S.** (Ch. 7)	**Mid-South Atlantic U.S.** (Ch. 7) **N. America** (Ch. 8)
Heat & Humidity	**Egypt** (Ch. 14) **India & Pakistan** (Ch. 16)		
Dryness	**Indonesia** (Ch. 22) **Tasmania** (Ch. 25)		
Heavy Precipitation	**China** (Ch. 18)		**Nigeria** (Ch. 13) **India** (Ch. 17)
Sunshine	**United Kingdom** (Ch. 10)		
Drought	**Canada** (Ch. 9) **Ethiopia and Southern Africa** (Ch. 15)		
Tropical Cyclones	**Western North Pacific** (Ch. 26)		
Wildfires	**Alaska** (Ch. 4)		
Sea Ice Extent		**Arctic** (Ch. 27)	
High Tide Floods	**Southeastern U.S.** (Ch. 6)		
Snowpack Drought	**Washington U.S.** (Ch. 5)		
TOTAL	23	2	5

	METHOD USED	Total Events
Heat	Ch. 2: **CMIP5 modeling** Ch. 11: **Observations; weather@home modeling** Ch. 12: **HadGEM3-A modeling** Ch. 15: **CMIP5 modeling** Ch. 19: **CMIP5 modeling with ROF; FAR** Ch. 20: **CMIP5 modeling with ROF; FAR** Ch. 21: **MIROC5-AGCM modeling** Ch. 22: **Observations; CMIP5 modeling** Ch. 23: **weather@home modeling; FAR** Ch. 24: **BoM seasonal forecast attribution system and seasonal forecasts**	12
Cold	Ch. 7: **Observations; CMIP5 modeling** Ch. 8: **AMIP (IFS model) modeling**	3
Heat & Humidity	Ch. 14: **weather@home modeling** Ch. 16: **Non-stationary EV theory; C20C+ Attribution Subproject**	2
Dryness	Ch. 22: **Observations; CMIP5 modeling** Ch. 25: **Observations; Modeling with CMIP5 and weather@home**	2
Heavy Precipitation	Ch. 13: **Observations; Modeling with CAM5.1 and MIROC5** Ch. 17: **Observations; Modeling with weather@home, EC-Earth and CMIP5** Ch. 18: **HadGEM3-A-N216 modeling; FAR**	3
Sunshine	Ch. 10: **Hadley Centre event attribution system built on the high-resolution version of HadGEM3-A**	1
Drought	Ch. 9: **Observations; CMIP5 modeling; Trend and FAR analyses** Ch. 15: **CMIP5 modeling, land surface model simulations, and statistical analyses**	2
Tropical Cyclones	Ch. 26: **GFDL FLOR modeling; FAR**	1
Wildfires	Ch. 4: **WRF-ARW optimized for Alaska with metric of fire risk (BUI) to calculate FAR**	1
Sea Ice Extent	Ch. 27: **OGCM modeling**	1
High Tide Floods	Ch. 6: **Tide-gauge data; Time-dependent EV statistical model**	1
Snowpack Drought	Ch. 5: **Observations; CESM1 modeling**	1
		30

ACRONYMS:

AMIP: Atmospheric Model Intercomparison Project
BoM: Bureau of Meteorology, Australia
BUI: Buildup Index
CAM: Community Atmosphere Model, http:www.cesm.ucar.edu
CESM: Community Earth System Model
CMIP: Coupled Model Intercomparison Project
FAR: Fraction of Attributable Risk
EC-EARTH: https://verc.enes.org/
EV: Extreme Value
GFDL FLOR: Geophysical Fluid Dynamics Laboratory Forecast version Low Ocean Resolution
GHCN: Global Historical Climatology Network
IFS: Integrated Forecast System
MIROC5–AGCM: Model for Interdisciplinary Research on Climate–Atmospheric General Circulation Model
OGCM: Ocean General Circulation Model
ROF: Regularized Optimal Fingerprinting
weather@home: http:www.climateprediction.net/weatherathome
WRF-ARW: Advanced Research (ARW) version of the Weather Research and Forecasting (WRF) model